Nanotechnology

Deutsche Ausgabe: DOI: 10.1002/ange.201500478
Internationale Ausgabe: DOI: 10.1002/anie.201500478

Hypoxia Induced by Upconversion-Based Photodynamic Therapy: Towards Highly Effective Synergistic Bioreductive Therapy in Tumors**

Yanyan Liu, Yong Liu, Wenbo Bu, Chao Cheng, Changjing Zuo, Qingfeng Xiao, Yong Sun, Dalong Ni, Chen Zhang, Jianan Liu, and Jianlin Shi**

Abstract: *Local hypoxia in tumors is an undesirable consequence of photodynamic therapy (PDT), which will lead to greatly reduced effectiveness of this therapy. Bioreductive pro-drugs that can be activated at low-oxygen conditions will be highly cytotoxic under hypoxia in tumors. Based on this principle, double silica-shelled upconversion nanoparticles (UCNPs) nanostructure capable of co-delivering photosensitizer (PS) molecules and a bioreductive pro-drug (tirapazamine, TPZ) were designed (TPZ-UC/PS), with which a synergetic tumor therapeutic effect has been achieved first by UC-based (UC-) PDT under normal oxygen environment, immediately followed by the induced cytotoxicity of activated TPZ when oxygen is depleted by UC-PDT. Treatment with TPZ-UC/PS plus NIR laser resulted in a remarkably suppressed tumor growth as compared to UC-PDT alone, implying that the delivered TPZ has a profound effect on treatment outcomes for the much-enhanced cytotoxicity of TPZ under PDT-induced hypoxia.*

PDT involves the administration of tumor-localizing photosensitizers (PSs) followed by the activation with a specific wavelength of light, and is clinically approved for the treatment of several types of solid cancer.[1] The antitumorigenic effects of PDT are achieved by the destruction of cells and tumor blood vessels by reactive oxygen species (ROS) (for example, singlet oxygen, $^1O_2$), which has a range of vascular effects, including transient vascular spasm, vascular stasis, the formation of thrombi, and permanent vessel occlusion.[2] Although vascular destruction reduces tissue oxygenation and thereby destroys tumors, the hypoxic microenvironment that consequently arises during PDT has been found to be responsible for the poor responses to radio- and chemotherapy, as well as to the following PDT itself, leading to considerably limited efficacy of PDT to tumors.[3] Moreover, induced hypoxia in tumors can stimulate the release of hypoxia inducible factor 1α and vascular endothelial growth factor, which can increase metastatic efficiency.[4] This negative consequence can be mitigated by developing advanced therapeutic approaches that overcome or even make use of the hypoxic microenvironment.

Hyperoxygenation by the inhalation of pure oxygen by patients at high pressures during PDT has been used to overcome tumor hypoxia; however, this method has only marginal benefits, because inhalated oxygen will not change the hypoxia efficiently owing to the temporary cessation of blood flow during PDT.[5] Combining PDT and photothermal therapy (PTT) can also enhance the therapeutic effect of PDT in tumors, since an appropriate level of hyperthermia can increase intratumoral blood flow and consequently promote tumor oxygenation. However, this method lacks specificity for hypoxic tissues and may induce an undesirable heat shock response during PTT.[6]

Fortunately, in spite of the greatly reduced therapeutic efficacy in PDT, the induced hypoxia can be exploited by introducing an agent that is selectively toxic to hypoxic cells so as to overcome the therapeutic resistance of the hypoxic tumors. Since bioreductive drugs will typically produce highly cytotoxic agents under hypoxic conditions, their cytotoxic activities can be triggered when used in conjunction with treatments that induce hypoxia.

Nevertheless, to potentiate the anticancer efficacy of PDT by using bioreductive drugs, an oxygen-deficit environment must be created for the bioreductive pro-drug activation.[7] The limited efficiency of conventional PDT is primarily due to the low tissue penetration of visible light and poor tumor accumulation of PS molecules.[8] The recent development of UCNPs capable of converting near-infared light (NIR) into UV-visible light enables the delivery of light to deep tissue and the use of PDT to treat previously inaccessible lesions.[9]

[*] Dr. Y. Liu, Prof. W. Bu, Dr. Q. Xiao, Dr. D. Ni, Dr. C. Zhang, Dr. J. Liu, Prof. J. Shi
State Key Laboratory of High Performance Ceramics and Superfine Microstructure, Shanghai Institute of Ceramics
Chinese Academy of Sciences
1295 Ding-xi Road, Shanghai 200050 (P.R. China)
E-mail: wbbu@mail.sic.ac.cn
jlshi@mail.sic.ac.cn
Prof. Y. Liu, Y. Sun
Cancer Research Institute
Shanghai Cancer Hospital, Fudan University
270 Dong-an Road, Shanghai 200032 (P.R. China)
Dr. C. Cheng, Dr. C. Zuo
Department of Nuclear Medicine
Changhai Hospital of Shanghai
168 Chang-hai Road, Shanghai 200433 (P.R. China)

[**] This work has been financially supported by the National Natural Science Foundation of China (Grant No. 51372260, 51132009, 21172043, 31370838), and the Scientific Research Foundation for the Returned Overseas Chinese Scholars from China State Education Ministry (No. N130204). Thanks to Linlin Zhang, Heliang Yao, Huaiyong Xing, Wenpei Fan, Zhaowen Cui, and Feng Chen from Shanghai Institute of Ceramics, Chinese Academy of Sciences for useful discussions.

Supporting information for this article is available on the WWW under http://dx.doi.org/10.1002/anie.201500478.

However, it is not known to date whether UC-based PDT is capable of creating strong enough hypoxia in tumors or not via the co-delivered PS molecules (silicon phthalocyanine dihydroxide, SPCD) to activate bioreductive pro-drugs, typically, for example, tirapazamine (TPZ).[10] In fact, TPZ can be stimulated by various intracellular reductase enzymes to generate a free-radical intermediate cytotoxic species. But this free radical tends to be rapidly oxidized back to the parent molecule, which has little effect on cells, while, under low-oxygen conditions, the highly reactive TPZ radical will remove hydrogen atoms from nearby macromolecules, causing them structural damage (Supporting Information, Figure S1).

Herein, a nanoplatform UC/PS composed of gadolinium (Gd^{3+})-doped UCNP core and double silica shells, that is, middle dense and outer mesoporous silica layers for efficient PS (SPCD) and pro-drug (TPZ) loading, has been constructed. The $NaYF_4$:Yb^{3+}/Er^{3+}/Gd^{3+} UCNPs were synthesized by a solvothermal method as previously reported.[11] The upconversion emissions of UCNPs at 652 nm overlay with the broad absorption spectrum of SPCD, allowing efficient energy transfer from the core to the PS (Figure 1a). To marry UCNP with PS in one unit, a modified reverse microemulsion method was employed (Figure 1b). NP-5 (IGEPAL CO-520) was first added to cyclohexane to form reverse micelles, and the hydrophobic UCNPs were then transferred to the micelle water pool after ligands exchange between oleate and NP-5. Following the sequential addition of PS and ammonia, tetraethyl orthosilicate was injected into the system and interacted with SPCD to yield a uniform core–shell structure with the UCNP core (Figure 1c) being coated with a dense silica shell to ensure the high payload and negligible leakage of PS (Figure 1d).[12] FTIR spectroscopy confirms the successful trapping of SPCD in the silica shell (Supporting Information, Figure S2). UC/PSs were finally obtained using an aqueous phase regrowth method to coat a mesoporous silica outer layer on the dense silica surface (Figure 1e) for TPZ loading, thereby endowing the nanostructure with the excellent functions of SPCD and TPZ co-delivery. TPZ (6 $\mu g\,mg^{-1}$) release from UC/PS was time- and pH-dependent (Supporting Information, Figure S3). Meanwhile, the inorganic silica component of UC/PS makes them highly biocompatible, and no significant cytotoxicity can be found to both cancer (HeLa) (Supporting Information, Figure S4) and healthy cells (NRK-52E and BRL) even at 1000 $\mu g\,mL^{-1}$ UC/PS (Supporting Information, Figure S5). Similarly, histological analyses of mice injected with 100 $mg\,kg^{-1}$ UC/PS reveal no pathological changes after 7 and 30 days (Supporting Information, Figure S6), confirming the satisfactory histocompatibility of UC/PS in vivo.

As we know that the production of ROS such as singlet oxygen ($^1O_2$) plays a major role in PDT. 980 nm laser irradiation on UC/PS resulted in an UC fluorescence emission that matched the absorption of SPCD moieties and caused intermolecular energy transfer to generate $^1O_2$. DPBF, whose fluorescence is irreversibly quenched by $^1O_2$, has long been used to detect this kind of ROS.[13] $^1O_2$ productions by the UC/PS, PS-unloaded UC, PS alone were investigated and compared under NIR laser irradiation. There are no changes in DPBF fluorescence in UC, PS, or the control group in which only the laser irradiation was used (Figure 2a), indicating that there is no $^1O_2$ generated when UC or PS was introduced solely. In contrast, the presence of UC/PS resulted in a high rate of DPBF fluorescence decay, evidencing the $^1O_2$ production.

For live cells, ROS production was examined by using 2′,7′-dichlorofluorescin diacetate (DCFH-DA). Once diffusing into cells, DCFH-DA is deacetylated by cellular esterases to a non-fluorescent compound, which is further oxidized by ROS into 2′,7′-dichlorofluorescein (DCF), which has characteristic excitation and emission maxima of 488 and 525 nm, respectively. There was little changes of DCF fluorescence signals detected by flow cytometry in cells treated with phosphate-buffered saline (PBS) or PS and then radiated with or without the 980 nm laser (Figure 2b). The results imply that NIR light alone or combined with PS cannot lead to the production of

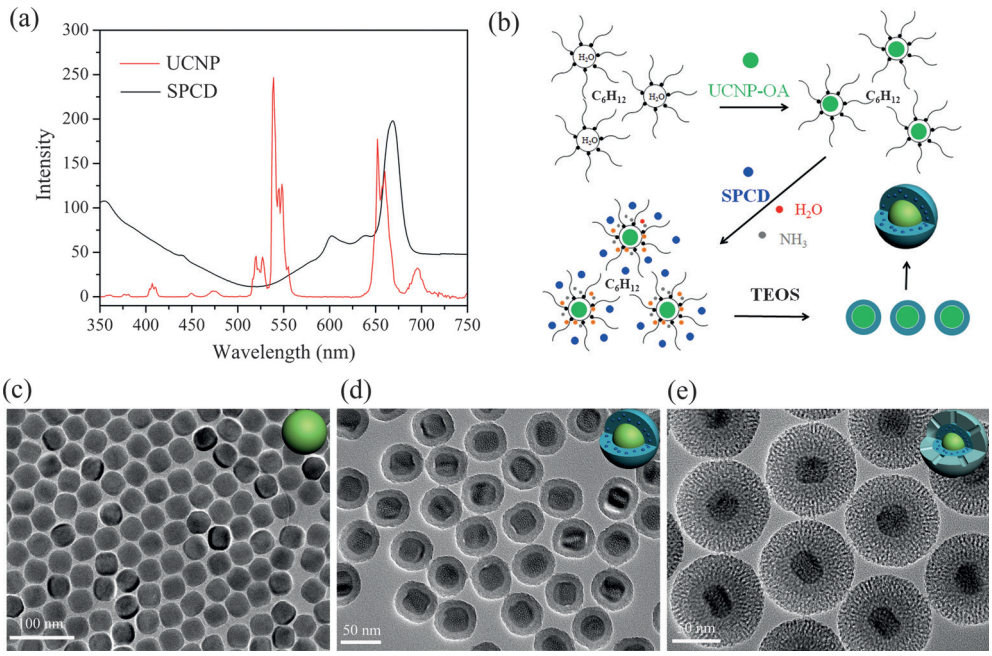

Figure 1. a) Fluorescence spectrum of UCNPs under 980 nm laser light excitation (red line) and UV/Vis absorption spectrum of SPCD (black line). b) Formation of UCNPs coated with PS-doped dense silica. c)–e) Representative transmission electron micrographs of UCNPs, UCNP coated with dense silica, and UCNPs coated with both dense and outer mesoporous silica shells (UC/PS).

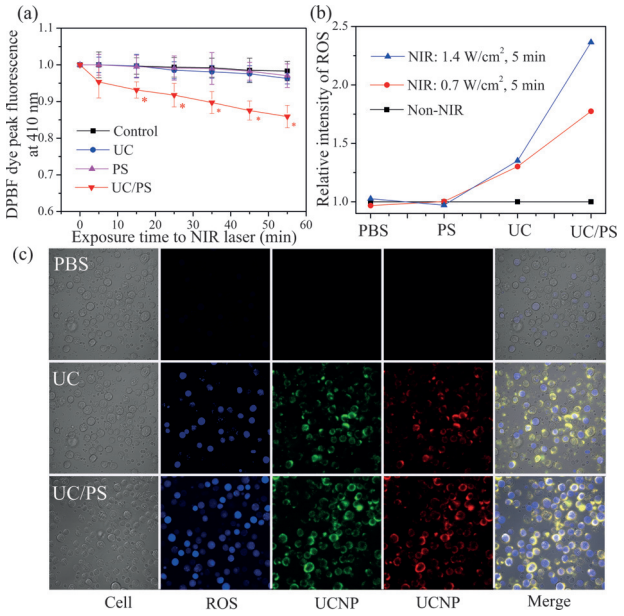

Figure 2. Enhanced PDT using UC/PS activated with single-wavelength laser light. a) Comparisons of $^1O_2$ production among control, UC, PS, and UC/PS groups following laser light irradiation at 980 nm (1.4 $W cm^{-2}$), as determined by the decay in DPBF fluorescence, which was measured at its peak intensity of 410 nm. Data represent mean ± SD ($n = 3$). b) ROS generation in cells treated with PDT, as assessed by flow cytometry. c) Confocal fluorescence images of cells after 980 nm laser light irradiation (1.4 $W cm^{-2}$, 5 min).

additional ROS, even at increased NIR laser power. In UC group, the development of reactive oxidative stress resulted from the impairment of the antioxidative capacity of a cell rather than the formation of intracellular ROS.

For cells cultured with UC/PS, intracellular fluorescence signals were markedly increased after exposure to 980 nm laser light. Incremental exposure to NIR energy leads to correspondingly increased fluorescence intensity, signaling an increase in ROS. The UC-based PDT effect was further assessed by confocal laser scanning microscopy. Figure 2c shows that the fluorescence intensity of ROS (blue color) detected using the fluorescein isothiocyanate (FITC) band pass filter was significantly higher in cells labeled with UC/PS than control cells treated with PBS or cultured with UC followed by laser irradiation under the similar cellular uptakes of both UC and UC/PS, as demonstrated by the intensified intracellular luminescence of UCNP detected using the 980 nm band pass filter. Together with the results of flow cytometry, the above evidence indicates that UC/PS under laser irradiation will produce ROS in cell.

The ability of TPZ-UC/PS in inducing cell death as compared to free TPZ was assessed in HeLa cells, as demonstrated in Figure 3. Considering the oxygen-dependent nature of PDT and TPZ, 10% pO_2 was set in cell apoptosis study to be as far as possible close to the physiological conditions.[14] Cell viability is similar upon treatment with PBS or free TPZ alone, with or without laser exposure, implying that laser irradiation and TPZ themselves have little detrimental effects. Once TPZ was loaded into UC/PS, the cell lethality was largely enhanced by the chemotherapeutic effect of TPZ. It is notable that cell viability is markedly reduced upon irradiation with 980 nm laser following treatment with either UC/PS or TPZ-UC/PS. The results confirm the effect of UC/PS as a PDT agent. Importantly, UC/PS-based PDT combined with TPZ-UC/PS shows great advantages over single UC-PDT, single TPZ-UC/PS or simple mixing of UC-PDT with free TPZ (Supporting Information, Figure S7). Thus, oxygen depletion by the UC-PDT photochemical reaction is sufficient to create hypoxia, and consequently, activate intracellular TPZ and increase cytotoxicity effectively.

Encouraged by the excellent biocompatiblity of UC/PS and the remarkable efficacy of the simple TPZ application with UC-PDT in vitro, we further performed the TPZ-PDT in vivo. Further evidence of the critical role of PDT-induced hypoxia in synergetically enhancing the anti-tumorigenic efficacy of TPZ was demonstrated by in vivo experiments.

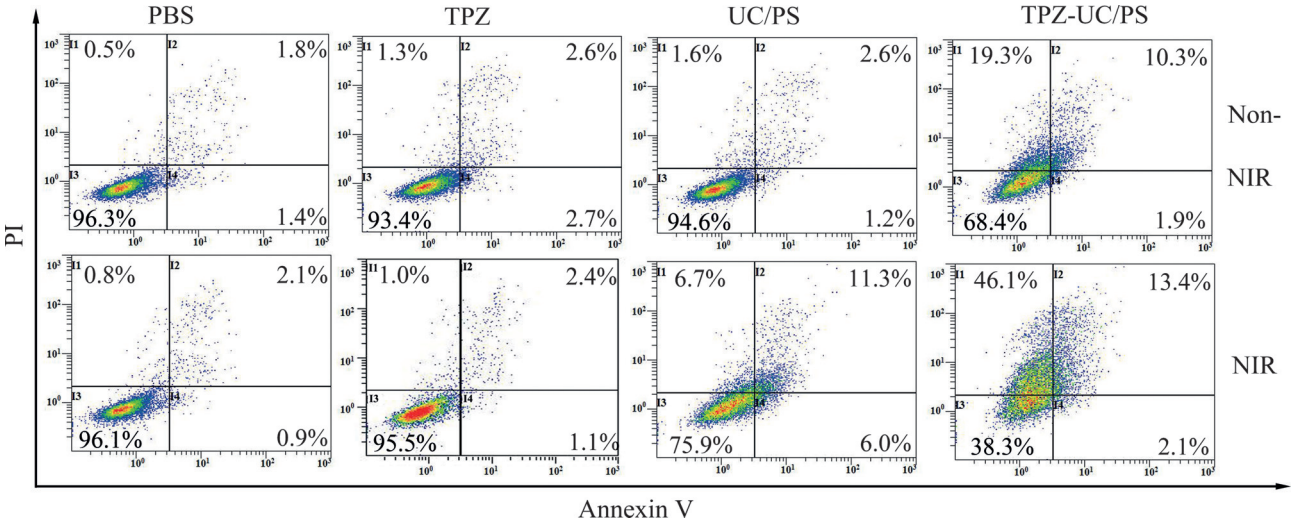

Figure 3. Flow cytometric analyses of cell apoptosis treated with PBS, TPZ (1.25 $\mu g mL^{-1}$), UC/PS (20.8 $\mu g mL^{-1}$), or TPZ-UC/PS (20.8 $\mu g mL^{-1}$, [TPZ] 1.25 $\mu g mL^{-1}$) at 10% pO_2. Non-NIR: unirradiated cells; NIR: cells irradiated with 980 nm laser light.

The chemical and physical properties of oxygen enable a wide variety of methods to locally detect oxygen content in vivo.[15] Here, ^{18}F-labeled MISO positron emission tomography (^{18}FMISO-PET) was employed in the quantitative analysis of the hypoxic sub-volumes in tumors based on the highly reproducible values of ^{18}FMISO uptake before and after UC-PDT.[16] We selected the median ^{18}FMISO tumor-to-background ratio (T/B) as discriminator for the oxygenation status of tumors,[17] with the T/B value ≥ 1.47 delineated as the hypoxic volume (HV). Because IR radiation on skin may have a local thermal effect that can alter the tumor microenvironment, tumors were laser-treated at 980 nm as a control. After 980 nm laser light irradiation, the T/B value remained stable below the median in the location of the tumors pre-treated with PBS or UC (Supporting Information, Figure S8), indicating the negligible effect of NIR on tissue oxygenation status. For tumors pre-injected with UC/PS shown in Figure 4a (i), T/B value in HeLa cell xenograft tumor significantly increased from 1.0 to 2.15 in 30 min starting from the treatment with 980 nm laser light irradiation on tumor, but no significant change of HV was observed for as long as two hours post-injection of UC/PS (Figure 4a (ii)). Thus, UC-PDT is capable of inducing strong local hypoxia in tumor, which makes TPZ-UC/PS a highly promising synergetic anticancer agent.

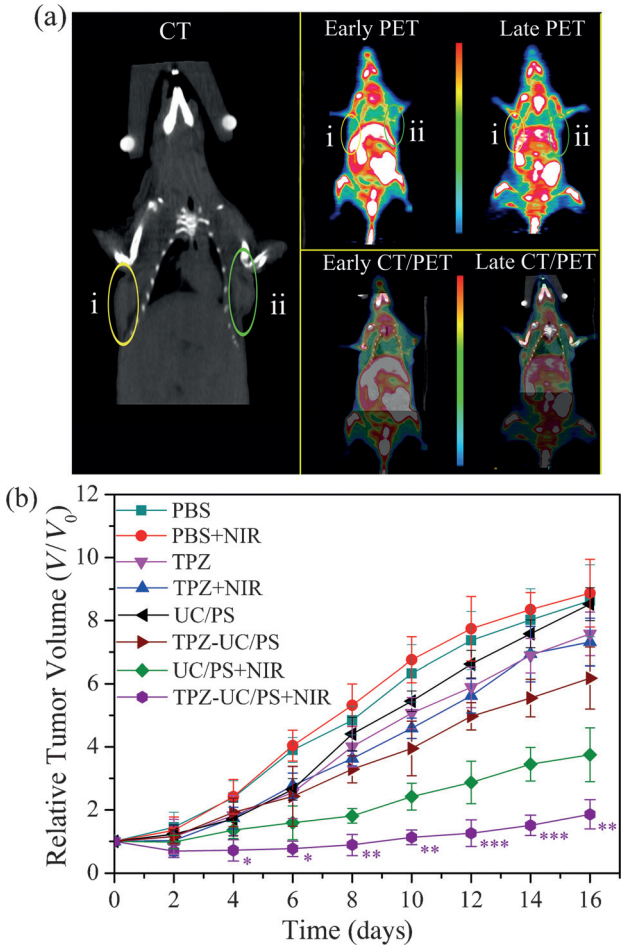

Figure 4. a) CT, early and late PET, and CT/PET imaging of HeLa cell xenograft tumors pre-treated with UC/PS after intravenous injection of ^{18}FMISO: i) tumor irradiated with the 980 nm laser light (1.4 W cm^{-2}, 15 min) between the 2 PET scans; ii) tumor without any further treatment. b) Time-dependent tumor growth curves obtained after the indicated in vivo treatments. The marked and sustained difference between groups (8) (TPZ-UC/PS + NIR) and (4) (TPZ-UC/PS) in the whole test of 16 days confirms the synergistic therapeutic effects of UC-PDT with TPZ-UC/PS. Statistical analysis was performed using the Student's two-tailed *t* test (*$P<0.05$, **$P<0.01$, and ***$P<0.001$).

To confirm the anticancer efficacy of TPZ-PDT in vivo, tumor-bearing nude mice (tumor diameter ca. 5 mm) were randomly divided into eight groups: 1) PBS alone, 2) UC/PS alone, 3) TPZ alone, 4) TPZ-UC/PS alone, 5) PBS + NIR, 6) UC/PS + NIR, 7) TPZ + NIR, and 8) TPZ-UC/PS + NIR. Excitingly, the most significant suppression on tumor growth was achieved in group (8), which was treated with TPZ-UC/PS and irradiated at 980 nm (Figure 4b). Combining the above results of ROS production and hypoxia generation by UC-PDT, such a remarkable in vivo tumor growth inhibition by group (8) indicates that the tumor hypoxia generated accompanying the ROS production is sufficiently strong to induce TPZ activation and suppress tumor growth, providing sound in vivo evidence for the synergistic effects of UC-PDT with bioreductive therapy using TPZ-UC/PS. TUNEL assays (Supporting Information, Figure S9) also confirm that this combined TPZ-PDT treatment can lead to marked cell apoptosis, further demonstrating the synergistic effects.

In summary, this study demonstrates that UC-PDT can be combined with bioreductive pro-drug for the NIR-induced synergetic therapy of tumors. UC-PDT generates a large amount of ROS in response to excitation by a 980 nm laser that kills cancer cells, and also plays an important role in the creation of hypoxic microenvironment by photochemical oxygen depletion and in inducing microvascular damage in tumors. Such a NIR-induced intratumoral hypoxia is sufficiently strong to potentiate the bioreductive therapy by the hypoxia-induced activation of co-delivered bioreductive pro-drug, demonstrating a high-effective synergistic tumor therapy. Thus, the combination of UC-PDT and TPZ has a great potential for treating a subset of patients with large or deep-seated tumors, and meanwhile the UCNP core can serve as a multifunctional matrix in bioimaging and NIR-controlled/MR-monitored drug release, and therefore can be exploited as a platform for multimodal imaging-guided therapeutics.[18]

Keywords: bioreductive pro-drugs · hypoxia · photodynamic therapy · synergetic therapy · upconversion nanoparticles

How to cite: *Angew. Chem. Int. Ed.* **2015**, *54*, 8105–8109
Angew. Chem. **2015**, *127*, 8223–8227

[1] M. Triesscheijn, P. Baas, J. H. M. Schellens, F. A. Stewart, *Oncologist* **2006**, *11*, 1034–1044.
[2] C. A. Robertson, D. H. Evans, H. Abraharnse, *J. Photochem. Photobiol. B* **2009**, *96*, 1–8.
[3] V. H. Fingar, T. J. Wieman, S. A. Wiehle, P. B. Cerrito, *Cancer Res.* **1992**, *52*, 4914–4921.
[4] a) M. I. Koukourakis, A. Giatromanolaki, J. Skarlatos, L. Corti, S. Blandamura, M. Piazza, K. C. Gatter, A. L. Harris, *Cancer Res.* **2001**, *61*, 1830–1832; b) S. Mitra, S. E. Cassar, D. J. Niles,

J. A. Puskas, J. G. Frelinger, T. H. Foster, *Mol. Cancer Ther.* **2006**, *5*, 3268 – 3274.
[5] a) Z. Huang, Q. Chen, A. Shakil, H. Chen, J. Beckers, H. Shapiro, F. W. Hetzel, *Photochem. Photobiol.* **2003**, *78*, 496 – 502; b) Q. Chen, Z. Huang, H. Chen, H. Shapiro, J. Beckers, F. W. Hetzel, *Photochem. Photobiol.* **2002**, *76*, 197 – 203.
[6] a) K. Hayashi, M. Nakamura, H. Miki, S. Ozaki, M. Abe, T. Matsumoto, T. Kori, K. Ishimura, *Adv. Funct. Mater.* **2014**, *24*, 503 – 513; b) P. Kalluru, R. Vankayala, C. S. Chiang, K. C. Hwang, *Angew. Chem. Int. Ed.* **2013**, *52*, 12332 – 12336; *Angew. Chem.* **2013**, *125*, 12558 – 12562.
[7] J. C. M. Bremner, G. E. Adams, J. K. Pearson, J. M. Sansom, I. J. Stratford, J. Bedwell, S. G. Bown, A. J. Macrobert, D. Phillips, *Br. J. Cancer* **1992**, *66*, 1070 – 1076.
[8] C. Wang, H. Q. Tao, L. Cheng, Z. Liu, *Biomaterials* **2011**, *32*, 6145 – 6154.
[9] N. M. Idris, M. K. Gnanasammandhan, J. Zhang, P. C. Ho, R. Mahendran, Y. Zhang, *Nat. Med.* **2012**, *18*, 1580 – U190.
[10] J. M. Brown, *Mol. Med. Today* **2000**, *6*, 157 – 162.
[11] F. Chen, W. B. Bu, S. J. Zhang, X. H. Liu, J. N. Liu, H. Y. Xing, Q. F. Xiao, L. P. Zhou, W. J. Peng, L. Z. Wang, J. L. Shi, *Adv. Funct. Mater.* **2011**, *21*, 4285 – 4294.
[12] F. Chen, S. J. Zhang, W. B. Bu, Y. Chen, Q. F. Xiao, J. N. Liu, H. Y. Xing, L. P. Zhou, W. J. Peng, J. L. Shi, *Chem. Eur. J.* **2012**, *18*, 7082 – 7090.
[13] Z. X. Zhao, Y. N. Han, C. H. Lin, D. Hu, F. Wang, X. L. Chen, Z. Chen, N. F. Zheng, *Chem. Asian J.* **2012**, *7*, 830 – 837.
[14] A. Carreau, B. El Hafny-Rahbi, A. Matejuk, C. Grillon, C. Kieda, *J. Cell. Mol. Med.* **2011**, *15*, 1239 – 1253.
[15] a) D. E. Achatz, R. J. Meier, L. H. Fischer, O. S. Wolfbeis, *Angew. Chem. Int. Ed.* **2011**, *50*, 260 – 263; *Angew. Chem.* **2011**, *123*, 274 – 277; b) C. S. Jin, J. F. Lovell, J. Chen, G. Zheng, *ACS Nano* **2013**, *7*, 2541 – 2550.
[16] a) D. Rischin, R. J. Hicks, R. Fisher, D. Binns, J. Corry, S. Porceddu, L. J. Peters, *J. Clin. Oncol.* **2006**, *24*, 2098 – 2104; b) K. Hendrickson, M. Phillips, W. Smith, L. Peterson, K. Krohn, J. Rajendran, *Radiother. Oncol.* **2011**, *101*, 369 – 375.
[17] S. Okamoto, T. Shiga, K. Yasuda, Y. M. Ito, K. Magota, K. Kasai, Y. Kuge, H. Shirato, N. Tamaki, *J. Nucl. Med.* **2013**, *54*, 201 – 207.
[18] a) D. L. Ni, J. W. Zhang, W. B. Bu, H. Y. Xing, F. Han, Q. F. Xiao, Z. W. Yao, F. Chen, Q. J. He, J. N. Liu, S. J. Zhang, W. P. Fan, L. P. Zhou, W. J. Peng, J. L. Shi, *ACS Nano* **2014**, *8*, 1231 – 1242; b) J. N. Liu, W. B. Bu, L. M. Pan, J. L. Shi, *Angew. Chem. Int. Ed.* **2013**, *52*, 4375 – 4379; *Angew. Chem.* **2013**, *125*, 4471 – 4475.

Received: January 18, 2015
Revised: April 2, 2015
Published online: May 26, 2015

